# Polyacetylenes from carrots (Daucus carota) improve glucose uptake in vitro in adipocytes and myotubes

El-Houri, Rime Bahij; Kotowska, Dorota Ewa; Christensen, Kathrine Bisgaard; Bhattacharya, Sumangala; Oksbjerg, Niels; Wolber, Gerhard; Kristiansen, Karsten; Christensen, Lars Porskjær

*Published in:*
Food & Function

*DOI (link to publication from Publisher):*
10.1039/c5fo00223k



*Publication date:*
2015

*Document Version*
Publisher's PDF, also known as Version of record

Organic & Biomolecular Chemistry

PAPER

View Article Online
View Journal | View Issue



CrossMark click for updates

Cite this: *Org. Biomol. Chem.*, 2015, **13**, 5115

# Thermal stability of G-rich anti-parallel DNA triplexes upon insertion of LNA and α-L-LNA†

Tamer R. Kosbar,[a,b] Mamdouh A. Sofan,[b] Laila Abou-Zeid[c] and Erik B. Pedersen*[a]

Received 17th March 2015,
Accepted 24th March 2015

DOI: 10.1039/c5ob00535c

www.rsc.org/obc

G-rich anti-parallel DNA triplexes were modified with LNA or α-L-LNA in their Watson–Crick and TFO strands. The triplexes were formed by targeting a pyrimidine strand to a putative hairpin formed by Hoogsteen base pairing in order to use the UV melting method to evaluate the stability of the triplexes. Their thermal stability was reduced when the TFO strand was modified with LNA or α-L-LNA. The same trend was observed when the TFO strand and the purine Watson–Crick strand both were modified with LNA. When all triad components were modified with α-L-LNA and LNA in the middle of the triplex, the thermal melting was increased. When the pyrimidine sequence was modified with a single insertion of LNA or α-L-LNA the $\Delta T_m$ increased. Moreover, increasing the number of α-L-LNA in the pyrimidine target sequence to six insertions, leads to a high increase in the thermal stability. The conformational S-type structure of α-L-LNA in anti-parallel triplexes is preferable for triplex stability.

## Introduction

DNA triplexes are formed when a DNA duplex containing a polypurine tract interacts with a third strand by means of specific hydrogen bonds in the major groove of the duplex. The formation of triple helices between DNA duplexes and external DNA single strands was introduced theoretically in 1953 by Pauling and Corey[1] and demonstrated experimentally by Rich and co-workers in 1957.[2]

Depending on the orientation of the third strand, triplexes are classified into two main categories: parallel and anti-parallel oriented triplexes.[3] The parallel-oriented triplexes (also named pyrimidine triplexes) are defined by three types of Hoogsteen base triads: d(T-A.T), protonated d(C-G.C$^+$) and d(C-G.G), where the last base refers to the Hoogsteen strand. The dot and hyphen refer to Hoogsteen and Watson–Crick binding, respectively, Fig. 1. Anti-parallel triplexes (also named purine triplexes) are classified by three reverse-Hoogsteen base triads: d(T-A.T), d(T-A.A) and d(C-G.G) as shown in Fig. 1.

Historically, guanine containing triplex forming oligonucleotides (G-rich TFOs) have been far less explored than TFOs based on pyrimidines (CT-TFOs). However, C-triplexes are unstable at neutral pH due to lacking protonation of cytosines which is required to form hydrogen bonds with the guanosines in the duplex. Therefore, it has been attempted to focus on pH-independent TFOs containing GA and/or GT nucleotides in order to design TFOs that combine DNA target-specificity with strong binding under physiological conditions.[4] However this approach is hampered by the tendency of G-rich TFOs to form highly stable aggregates, mostly in the

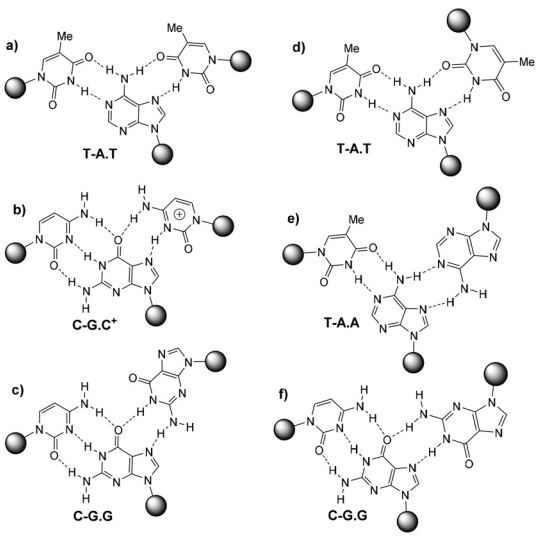


**Fig. 1** First column: Hoogsteen pairings found in parallel triplexes (a, b and c), second column: reverse Hoogsten pairings found in anti-parallel triplexes (d, e and f).

[a]*Nucleic Acid Center, Department of Physics, Chemistry, and Pharmacy, University of Southern Denmark, Campusvej 55, 5230 Odense M, Denmark. E-mail: erik@sdu.dk; Fax: +45 66158780*
[b]*Department of Chemistry, Faculty of Science, Damietta University, 34517 New Damietta, Egypt*
[c]*Department of Pharmaceutical Organic Chemistry, Faculty of Pharmacy, Mansoura University, 35516 Mansoura, Egypt*
†Electronic supplementary information (ESI) available. See DOI: 10.1039/c5ob00535c

form of inter- or intramolecular G-quadruplexes, thus preventing triplex formation.[5–7]

Several strategies have been developed to avoid the self-aggregation of G-rich TFOs, some of them depend on formation of short duplexes on the 3′- or 5′-ends of G-rich TFOs,[8] replacement of phosphodiester internucleotide bonds with positively charged phosphoramidites[9] or modification of the TFO strand with twisted intercalating nucleic acid monomer (TINA) which effectively circumvents guanine-mediated self-association of G-rich anti-parallel TFOs.[10] Also, 8-aminoguanine has a unique profile as a molecule showing simultaneous strong triplex-stabilization and quadruplex-destabilization.[11] The introduction of 8-aminoguanine into triplex-forming oligonucleotides seems preferable compared to other modified purines like 6-thioguanine,[6,12] 9-deazaguanine,[13] 7-deazaxanthine,[14] 6-thio-7-deazaguanine,[15] or 7-chloro-7-deazaguanine.[16] Although they were found to inhibit quadruplex formation, there was no improvement on triplex stability.

LNA (Locked Nucleic Acid) is a nucleotide modification (Fig. 2) with a 2′-*O*, 4′-*C*-methylene linked bicyclic ribonucleoside locked in an 3′-*endo* conformation. This preorganizes the sugar-phosphate backbone to facilitate a more efficient stacking of the nucleobases.[17] α-L-LNA (α-L-*ribo* configured LNA, Fig. 2) is a diastereoisomer of LNA. Like LNA it improves stability against nucleases and induces high affinity towards DNA and especially RNA complements when incorporated into oligonucleotides.[18,19] α-L-LNA can be described as a DNA mimic with respect to helical structure, whereas LNA is an RNA mimic.[20,21]

It was reported that incorporation of LNA-T or LNA-C in the homo-pyrimidine strand significantly increased the binding affinity of TFOs,[22–24] but unexpectedly, a continuous stretch of 12–13 LNA-T and LNA-C monomers in the TFO decreased the affinity dramatically so that no triplex formation could be detected.[24] There is also a report claiming reverse Hoogsteen hydrogen bonding with (G,A)- and (G,T)-containing LNA-TFOs to be disfavored, but without reporting the corresponding experimental data.[25] In contrast to LNA-TFOs, the fully modified α-L-LNA-TFO forms a stable parallel triplex with a DNA duplex.[26]

Herein, G-rich triplexes were modified with LNA and α-L-LNA in the TFO and Watson–Crick strands. To the best of our knowledge this is the first report describing the incorporation of α-L-LNA into anti-parallel TFOs.

## Results and discussion

In this study, we were dealing with two hairpins that target a pyrimidine strand to form the triplexes **ON1** and **ON2**. These two triplexes were taken from a previous anti-parallel triplex study, where the linking between the Watson–Crick polypurine and the reverse-Hoogsteen strands was done by a tetrathymidine loop,[27] Fig. 3.

In our hands the triplexes **ON1** and **ON2** showed melting temperatures at 61.5 °C and 60.5 °C, respectively (Table 1). For **ON1** this is close to the previously reported temperature at 62.7 °C.[27] The single strands forming hairpins did not show any melting and melting was observed only when the putative hairpins were mixed with the pyrimidine target sequences. This observation is in agreement with the previous finding that reverse-Hoogsteen hairpins are not fully preorganized before binding to the third strand.[27] Interestingly, the control duplexes formed by Watson–Crick 11-mer and corresponding polypurine strand **ON26** and **ON29** (with scrambled anti-parallel strand) melted at lower temperatures (47–48 °C, Table 2).

Firstly, we modified the TFO with adenine-LNA ($\mathbf{A^L}$), guanine-LNA ($\mathbf{G^L}$), thymine-LNA ($\mathbf{T^L}$) or thymine-α–L-LNA ($\mathbf{T^\alpha}$),

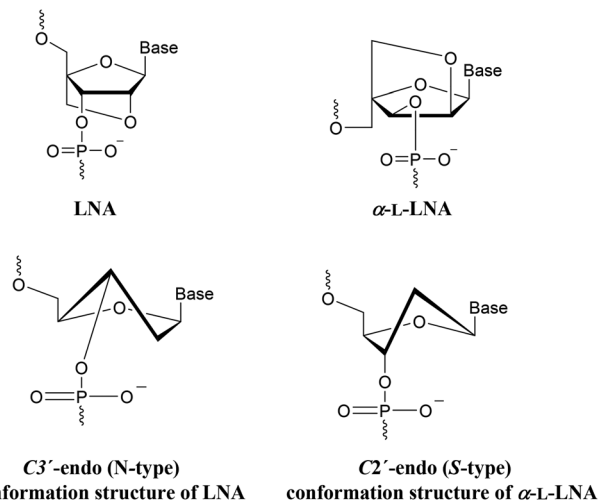


Fig. 2 Structure of LNA ($T^L$, $C^L$, $A^L$, $G^L$) and α-L-LNA ($T^\alpha$, $C^\alpha$) nucleotide monomers.

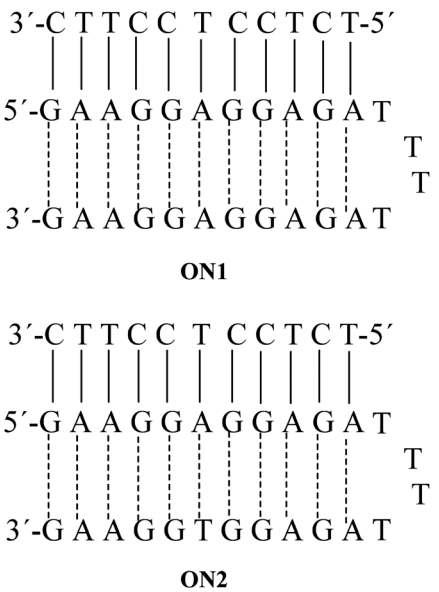


Fig. 3 Anti-parallel triplexes **ON1** and **ON2**.

**Table 1** Thermal melting $T_m$ [°C] of triplexes melting **ON1–ON25**, taken from UV melting curves ($\lambda$ = 260 nm) recorded in 10 mM sodium cacodylate, 50 mM $MgCl_2$, and 0.1 mM EDTA buffer solution at pH 7.2[a]

| | Watson–Crick | Hairpin | | | $\Delta T_m$ (°C) | |
|---|---|---|---|---|---|---|
| ON | Target | Watson–Crick | TFO | $T_m$ (°C) | Ref. **ON1** | Ref. **ON2** |
| 1 | 5′TCTCCTCCTTC3′ | 5′GAAGGAGGAGA-TTTT-AGAGGAGGAAG3′ | | 61.5 | | |
| 2 | 5′TCTCCTCCTTC3′ | 5′GAAGGAGGAGA-TTTT-AGAGGTGGAAG3′ | | 60.5 | | |
| 3 | 5′TCTCCTCCTTC3′ | 5′GAAGGAGGAGA-TTTT-AGAGG$^{L}$AGGAAG3′ | | 54.5 | −7.0 | |
| 4 | 5′TCTCCTCCTTC3′ | 5′GAAGGAGGAGA-TTTT-AGAGGA$^{L}$GGAAG3′ | | 56.5 | −5.0 | |
| 5 | 5′TCTCCTCCTTC3′ | 5′GAAGGAGGAGA-TTTT-AGAGGT$^{L}$GGAAG3′ | | 53.5 | | −7.0 |
| 6 | 5′TCTCCTCCTTC3′ | 5′GAAGGAGGAGA-TTTT-AGAGGT$^{\alpha}$GGAAG3′ | | 55.0 | | −5.5 |
| 7 | 5′TCTCCTCCTTC3′ | 5′GAAGGAG$^{L}$GAGA-TTTT-AGAGGAGGAAG3′ | | 60.5 | −1.0 | |
| 8 | 5′TCTCCTCCTTC3′ | 5′GAAGGA$^{L}$GGAGA-TTTT-AGAGGAGGAAG3′ | | 62.0 | 0.5 | |
| 9 | 5′TCTCCTCCTTC3′ | 5′GAAGGA$^{L}$GGAGA-TTTT-AGAGGA$^{L}$GGAAG3′ | | 58.5 | −3.0 | |
| 10 | 5′TCTCCTCCTTC3′ | 5′GAAGGAG$^{L}$GAGA-TTTT-AGAGG$^{L}$AGGAAG3′ | | 56.5 | −5.0 | |
| 11 | 5′TCTCCTCCTTC3′ | 5′GAAGGA$^{L}$GGAGA-TTTT-AGAGGT$^{\alpha}$GGAAG3′ | | 58.5 | | −2.0 |
| 12 | 5′TCTCCT$^{\alpha}$CCTTC3′ | 5′GAAGGA$^{L}$GGAGA-TTTT-AGAGGT$^{\alpha}$GGAAG3′ | | 64.0 | | 3.5 |
| 13 | 5′TCTCCT$^{L}$CCTTC3′ | 5′GAAGGA$^{L}$GGAGA-TTTT-AGAGGT$^{\alpha}$GGAAG3′ | | 63.5 | | 3.0 |
| 14 | 5′TCTCCT$^{\alpha}$CCTTC3′ | 5′GAAGGAGGAGA-TTTT-AGAGGT$^{\alpha}$GGAAG3′ | | 60.0 | | −0.5 |
| 15 | 5′TCTCCT$^{L}$CCTTC3′ | 5′GAAGGAGGAGA-TTTT-AGAGGT$^{L}$GGAAG3′ | | 57.5 | | −3.0 |
| 16 | 5′TCTCCT$^{\alpha}$CCTTC3′ | 5′GAAGGAGGAGA-TTTT-AGAGGT$^{L}$GGAAG3′ | | 59.0 | | −1.5 |
| 17 | 5′TCTCCT$^{L}$CCTTC3′ | 5′GAAGGAGGAGA-TTTT-AGAGGTGGAAG3′ | | 64.0 | | 3.5 |
| 18 | 5′TCTCCT$^{\alpha}$CCTTC3′ | 5′GAAGGAGGAGA-TTTT-AGAGGTGGAAG3′ | | 64.5 | | 4.0 |
| 19 | 5′TCT$^{L}$CCT$^{L}$CCT$^{L}$TC3′ | 5\GAAGGAGGAGA-TTTT-AGAGGTGGAAG3′ | | 69.5 | | 9.0 |
| 20 | 5′TCT$^{\alpha}$CCT$^{\alpha}$CCT$^{\alpha}$TC3′ | 5′GAAGGAGGAGA-TTTT-AGAGGTGGAAG3′ | | 72.0 | | 11.5 |
| 21 | 5′TCTCC$^{L}$TCCTTC3′ | 5′GAAGGAGGAGA-TTTT-AGAGGTGGAAG3′ | | 66.0 | | 5.5 |
| 22 | 5′TC$^{L}$TCC$^{L}$TCC$^{L}$TTC3′ | 5′GAAGGAGGAGA-TTTT-AGAGGTGGAAG3′ | | 73.5 | | 13.0 |
| 23 | 5′TCTCC$^{\alpha}$TCCTTC3′ | 5′GAAGGAGGAGA-TTTT-AGAGGTGGAAG3′ | | 66.5 | | 6.0 |
| 24 | 5′TC$^{\alpha}$TCC$^{\alpha}$TCC$^{\alpha}$TTC3′ | 5′GAAGGAGGAGA-TTTT-AGAGGTGGAAG3′ | | 76.0 | | 15.5 |
| 25 | 5′TC$^{\alpha}$T$^{\alpha}$CC$^{\alpha}$T$^{\alpha}$CC$^{\alpha}$T$^{\alpha}$TC3′ | 5′GAAGGAGGAGA-TTTT-AGAGGTGGAAG3′ | | 82.0 | | 21.5 |

[a] **C** = cytosine, **C$^{L}$** = 5-methylcytosine LNA, **C$^{\alpha}$** = 5-methylcytosine $\alpha$-L-LNA.

**Table 2** Thermal melting $T_m$ [°C] data of duplexes melting **ON26–ON36**, taken from UV melting curves ($\lambda$ = 260 nm) recording in 10 mM sodium cacodylate, 50 mM $MgCl_2$, and 0.1 mM EDTA buffer solution at pH 7.2[a]

| | | | | $\Delta T_m$ (°C) | |
|---|---|---|---|---|---|
| ON | Pyrimidine sequence | Purine sequence | $T_m$ (°C) | Ref. **ON26** | Ref. **ON29** |
| 26 | 5′TCTCCTCCTTC3′ | 5′GAAGGAGGAGA3′ | 48.0 | | |
| 27 | 5′TCTCCTCCTTC3′ | 5′GAAGGA$^{L}$GGAGA3′ | 53.5 | 5.5 | |
| 28 | 5′TCTCCTCCTTC3′ | 5′GAAGGAG$^{L}$GAGA3′ | 53.5 | 5.5 | |
| 29 | 5′TCTCCTCCTTC3′ | 5′GAAGGAGGAGA-TTTT-GAGAGGAAAGA3′ | 47.0 | | |
| 30 | 5′TCTCCTCCTTC3′ | 5′GAAGGA$^{L}$GGAGA-TTTT-GAGAGGAAAGA3′ | 51.0 | | 3.0 |
| 31 | 5′TCTCCTCCTTC3′ | 5′GAAGGAG$^{L}$GAGA-TTTT-GAGAGGAAAGA3′ | 51.0 | | 3.0 |
| 32 | 5′TCTCCT$^{\alpha}$CCTTC3′ | 5′GAAGGAGGAGA3′ | 51.0 | 3.0 | |
| 33 | 5′TCT$^{\alpha}$CCT$^{\alpha}$CCT$^{\alpha}$TC3′ | 5′GAAGGAGGAGA3′ | 56.0 | 8.0 | |
| 34 | 5′TCTCC$^{\alpha}$TCCTTC3′ | 5′GAAGGAGGAGA3′ | 54.0 | 6.0 | |
| 35 | 5′TC$^{\alpha}$TCC$^{\alpha}$TCC$^{\alpha}$TTC3′ | 5′GAAGGAGGAGA3′ | 62.0 | 14.0 | |
| 36 | 5′TC$^{\alpha}$T$^{\alpha}$CC$^{\alpha}$T$^{\alpha}$CC$^{\alpha}$T$^{\alpha}$TC3′ | 5′GAAGGAGGAGA3′ | 68.0 | 20.0 | |

[a] **C** = cytosine, **C$^{\alpha}$** = 5-methylcytosine α-L-LNA.

but unfortunately, the $T_m$ was decreased in all cases. The $\Delta T_m$ was −7 °C in case of **G$^{L}$** (**ON3**) and **T$^{L}$** (**ON5**). In case of **A$^{L}$** (**ON4**) and **T$^{\alpha}$** (**ON6**) it was −5 °C and −5.5 °C, respectively. This confirms the previously published statement that LNA in the TFO destabilize the anti-parallel triplex.[25] Also, we tried to modify the Watson–Crick part in the middle with LNA. However, the $T_m$ increased only 0.5 °C with **A$^{L}$** (**ON8**) and decreased 1 °C with **G$^{L}$** (**ON7**), Table 1.

Moreover, when the TFO and Watson–Crick parts both were modified with LNA in the middle of the sequence, the $T_m$ also decreased, but we noticed that the decrease in the $T_m$ is much lower than in case of LNA in the TFO only. For example, when we compared the $T_m$ values of **ON3** and **ON10**, we observed that the $T_m$ increased about 2 °C (from 54.5 °C to 56.5 °C, Table 1). The same trend in $T_m$ values was observed when comparing **ON4** with **ON9** and **ON6** with **ON11**.

One insertion of $\mathbf{T}^{\alpha}$ in the pyrimidine target sequence and in the TFO part decreased the thermal stability of the anti-parallel triplex by only 0.5 °C (**ON14**). In contrast, using $\mathbf{T}^{\mathbf{L}}$ in the same two positions the decrease in $T_m$ was 3 °C (**ON15**).

Interestingly, the stability of anti-parallel triplex increased, when all the three strands were modified with LNA. The $T_m$ data revealed that, the difference in $T_m$ values between triplexes **ON11** with LNA in TFO and Watson–Crick parts and **ON12** with LNA in all three parts is 5.5 °C ($\Delta T_m$ changed from −2 °C to 3.5 °C, Table 1). We assume that, this dramatic increase in the $T_m$ when the pyrimidine target sequence was modified with LNA, is due to increased stacking between the nucleobases in the duplex part (see molecular modeling section).

It has been reported that 2–4 insertions of twisted intercalating nucleic acid (TINA) in the TFO strand increase the stability of G-rich TFOs and prevent G-quadruplexes formation. The pyrene moiety is positioned inside the DNA duplex between base pairs during the triplex formation which increases the stacking in the duplex part.[10] This means that, the stability of anti-parallel TFO depends on the stacking in Watson–Crick duplex. Based on this observation, it was found interesting to modify only the pyrimidine target sequence with LNA and therefore the triplexes **ON17–ON25** were investigated. As expected, one insertion of LNA in the pyrimidine target sequence increases the $T_m$ by 4 °C in case of **ON18** with $\mathbf{T}^{\alpha}$ and by 3.5 °C in case of **ON17** with $\mathbf{T}^{\mathbf{L}}$. When 5-methylcytosine (**C**) was used as base in LNA and α-L-LNA, it was found that one insertion of α-L-LNA-C ($\mathbf{C}^{\alpha}$) in **ON23** and LNA-C ($\mathbf{C}^{\mathbf{L}}$) in **ON21** increase the melting temperature by 6 °C and 5.5 °C, respectively.

The effect seems additive since three insertions of $\mathbf{T}^{\alpha}$ in **ON20** or $\mathbf{T}^{\mathbf{L}}$ in **ON19** gave higher thermal stabilities with $\Delta T_m$ = 11.5 °C and 9 °C, respectively, compared to the wild type **ON2** (Table 1). The same trend was observed for three modifications $\mathbf{C}^{\alpha}$ (**ON24**) and $\mathbf{C}^{\mathbf{L}}$ (**ON22**) in the pyrimidine target sequence, $\Delta T_m$ = 15.5 °C and 13 °C, respectively (Table 1), reflecting higher melting temperatures for LNAs-C than for LNAs-T.

From the results, we noticed that α-L-LNA gave higher thermal stability in all cases compared to LNA. Concerning the conformational structure of anti-parallel triplexes, it has been reported that only S-type (south-type) sugars are favorable for the anti-parallel triplex.[28] On the other hand, It has been found that the conformation structure of the furanose ring in α-L-LNA is the S-type,[20] and this explain that α-L-LNA is more suitable for anti-parallel TFOs. This encouraged us to increase the number of α-L-LNA in the pyrimidine target sequence to six α-L-LNA nucleobases using three $\mathbf{C}^{\alpha}$ and three $\mathbf{T}^{\alpha}$ (**ON25**) which leads to a significant increase in the thermal stability with $\Delta T_m$ = 21.5 °C (Table 1).

In order to be sure that the TFO strand is contributing to the stability of the target complex, the corresponding duplexes **ON26–ON36** were considered. In all cases the $T_m$ was lower than for the corresponding triplexes. This was also the case for **ON29–ON31** with a mismatched dangling TFO part (Table 2).

## CD measurements

All the triplexes with or without modification of **T** in the pyrimidine target sequence showed a positive band at 270 nm and a negative band at 242 nm in their CD spectra. This means that the spectra of **ON12–ON20** with $\mathbf{T}^{\mathbf{L}}$ and $\mathbf{T}^{\alpha}$ are in agreement with the CD spectra of (G,A) anti-parallel triplexes,[29] Fig. 4a.

From Fig. 4b it can be seen that there is an indication of shoulders on both sides of the 270 nm band in the CD spectra of ON21 with one $\mathbf{C}^{\mathbf{L}}$ insertion in the target sequence and of ON23 with one $\mathbf{C}^{\alpha}$ insertion in the target sequence. When the number of $\mathbf{C}^{\mathbf{L}}$ or $\mathbf{C}^{\alpha}$ was increased, the CD spectra changed more for ON22, ON24 and ON25 and shoulders appeared clearly at 255 nm and 285 nm.

The increasing number of $\mathbf{C}^{\mathbf{L}}$ and $\mathbf{C}^{\alpha}$ in the target sequence may change the conformation of the duplex part of the triplex. When inserted into a duplex, LNA is known to change the flanking nucleotides into an N-type sugar conformation.[30] In fact, the shoulders in the CD spectra of **ON21–ON25** corresponds to the main bands observed by Shibata *et al.* in an

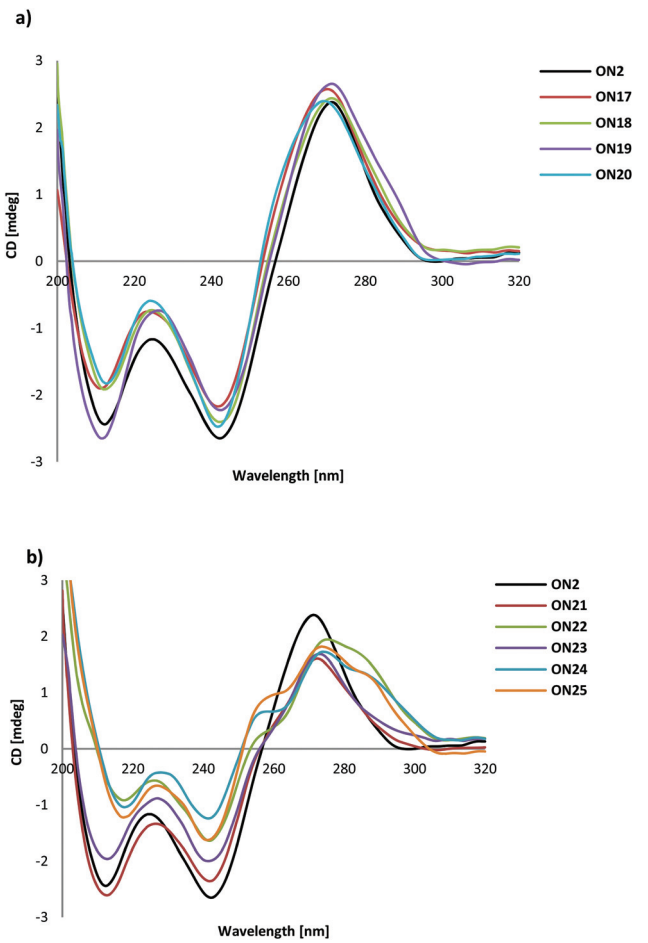


**Fig. 4** (a) Typical examples of CD spectra of **ON2** and **ON17–ON19** with $\mathbf{T}^{\mathbf{L}}$ and $\mathbf{T}^{\alpha}$. (b) CD spectra of **ON2** and **ON21–25** with $\mathbf{C}^{\mathbf{L}}$ and $\mathbf{C}^{\alpha}$.

anti-parallel triplex with a higher G/A ratio and with 5-aminomethyl modification for one of the thymidines.[31]

## Molecular modeling

In order to understand the binding and stacking properties of the anti-parallel triplex modified with LNA and α-L-LNA, we decided to get insight into their structures *via* molecular modeling studies. An AMBER* force field in Macro Model 9.1, molecular modeling was used to generate representative low energy structures of the modified structures with LNA and α-L-LNA at different positions in the Watson–Crick and TFO parts of the triplexes. Patel's structure of the anti-parallel triplex d(TGGTGGT) which contains d(G-GC) and (T-AT) triads (PDB entry pdb134d)[32] was used and modified with LNA and α–L-LNA.

The results showed that, multi insertion of α-L-LNA ($\mathbf{T^{\alpha}}$ and $\mathbf{C^{\alpha}}$) in the pyrimidine target sequence increase the stacking between the nucleobases in the three strands of the anti-parallel triplex which reflects the high thermal stability of **ON25** (Fig. 5a).

In contrast, a larger distortion of the triplex structure was observed when the TFO strand was modified with $\mathbf{T^{L}}$ (Fig. 5d), the LNA moiety and some other TFO's nucleobases were forced to twist out of plane of Watson–Crick base pair which is weakening the stacking interactions with the TFO nucleobases and the binding with the duplex part. The same trend was observed in case of $\mathbf{T^{\alpha}}$ in the TFO strand (Fig. 5c). This explains the lower thermal stability of ON5 and ON6.

However, when the TFO, Watson–Crick and the target strands were modified with $\mathbf{T^{\alpha}}$, $\mathbf{A^{L}}$ and $\mathbf{T^{\alpha}}$, respectively (Fig. 5b), the triplex structure was undisturbed and the $\mathbf{T^{\alpha}}$-nucleobase in the TFO strand hybridized nicely to the nucleobase $\mathbf{A^{L}}$ in the Watson–Crick duplex, thereby explaining the increase in stability when the three strands were modified with α-L-LNA and LNA (**ON12**).

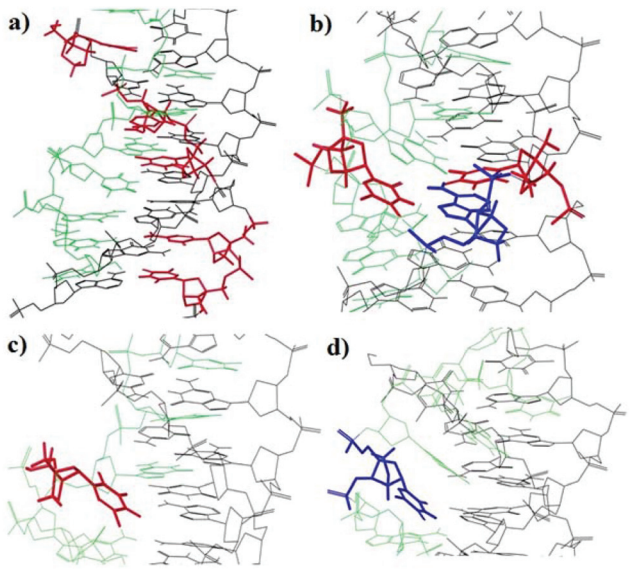


**Fig. 5** Representative low-energy conformations of anti-parallel triplex (TFO the green color and Watson–Crick duplex the black color) containing insertion of LNA (blue color) and α-L-LNA (red color) produced by AMBER* calculations (a) α-L-LNA-T and α-L-LNA-C insertions in the target sequence, (b) α-L-LNA-T, LNA-A and α-L-LNA-T insertions as a base triplet in the TFO and duplex parts of the triplex. (c) α-L-LNA-T insertion in the TFO. (d) LNA-T insertion in the TFO.

## Conclusion

The stability of anti-parallel triplexes was increased when the pyrimidine sequence was modified with LNA ($\mathbf{C^{L}}$ and $\mathbf{T^{L}}$) and α-L-LNA ($\mathbf{C^{\alpha}}$ and $\mathbf{T^{\alpha}}$). Molecular model building is supportive of base stacking between the nucleobases in the duplex part. However, α-L-LNA gave higher thermal stability in all cases when compared to LNA, because the conformational S-type structure of α-L-LNA corresponding to the sugar conformation in anti-parallel triplexes is preferable for triplex stability.[28] A substantial increase in thermal stability was also observed when a base triad was fully modified with LNA and α-L-LNA ($\mathbf{T^{\alpha}}$,$\mathbf{A^{L}}$,$\mathbf{T^{\alpha}}$ or $\mathbf{T^{L}}$,$\mathbf{A^{L}}$,$\mathbf{T^{\alpha}}$) in contrast to modification in the purine strands only. When only the purine TFO strand was modified, the triplex stability was reduced. According to molecular modeling, this is due to reduced stacking in the TFO part. We think that our findings about antiparallel triplex stability could be important for developing a strategy for strand invasion by clamping a G-rich purine strand in a duplex. This corresponds to a reported strand invasion method based on formation of a parallel triplex on an A-rich sequence.[33]

## Experimental section

### General

All locked nucleoside amidites were purchased from Exiqon. Unmodified oligonucleotides were purchased from Sigma on a 0.2 mmol scale; the purity was checked by ion-exchange chromatography and MALDI-TOF mass spectrometry.

### Oligonucleotide synthesis

Modified oligonucleotides were synthesized in 0.2 mmol scale on 500 Å CPG supports using ExpediteTM Nucleic Acid Synthesis System model 8909 from Applied Biosystems. Standard procedures were used for the coupling of commercial phosphoramidites, whereas modified phosphoramidites, LNA-A ($\mathbf{A^{L}}$), LNA-G ($\mathbf{G^{L}}$), LNA-T ($\mathbf{T^{L}}$), α-L-LNA-T ($\mathbf{T^{\alpha}}$), 5-methylcytosine types LNA-C ($\mathbf{C^{L}}$) and α-L-LNA-C ($\mathbf{C^{\alpha}}$), were coupled with 1*H*-tetrazole in $CH_3CN$ as an activator and an extended coupling time (15 min), the coupling efficiency was higher than 95% in all cases. ONs were de-protected and cleaved from the CPG support with 32% aq. $NH_3$ (1 mL) and left at 55 °C for 20 h. ONs were purified as DMT-on ONs by Reversed phase-HPLC using: (1) *Column*: XBridge OST C18, 19 × 1000 mm, 5 μm +

precolumn: XBridge 10 × 10 mm, 5 μm, the temperature of column oven was 50 °C. (2) Buffers: [Buffer A: 0.05 M TEAA (triethyl ammonium acetate) pH 7.4; Buffer B: 75% MeCN/25% Buffer A], flow: 5 mL $min^{-1}$.

ONs were submitted to DMT deprotection with 80% aq. AcOH (100 μL) for 30 min, followed by addition of doubly filtered $H_2O$ (100 μL), aq. AcONa (5 M, 15 μL), and aq. $NaClO_4$ (5 M, 15 μL) before precipitation from pure acetone (1 mL). Molecular masses of all modified ONS were confirmed by MALDI-TOF analysis on a Ultraflex II TOF/TOF system from Bruker (a MALDI-LIFT system) with HPA matrix (10 mg 3-hydroxypicolinic acid, in 50 mM ammonium citrate/70% MeCN). The purity of the final ONs were found to be ~99% when checked by ion-exchange chromatography using *La-Chrom* system from *Merck Hitachi* on *Dionex DNA Pac Pa-100*, 4 × 250 mm anal. column. Buffers: [Buffer A: $H_2O$ Milli-Q; Buffer B: 1 *M* $NaClO_4$; Buffer C: 25 m*M* Tris-Cl, pH 8.0; Buffer D: MeCN], Flow: 1 mL $min^{-1}$.

### Thermal denaturation studies

Thermal melting measurements were performed on a Perkin-Elmer UV/VIS spectrometer Lambda 35 fitted with a PTP-6 temperature programmer. Melting experiments were performed on equimolar amounts of the appropriate oligonucleotides (target sequence and hairpin) (3 μM) in a buffer solution consisting of sodium cacodylate (10 mM), EDTA (0.1 mM), and $MgCl_2$ (50 mM) at pH 7.2. The solutions were heated to 90 °C then cooled down slowly to room temperature, and were then kept at this temperature for 2 h. The absorbance of the formed triplexes was measured at 260 nm with a heating rate of 0.5 °C $min^{-1}$. The melting temperature ($T_m$) was determined as the maximum of the first derivative plots of the melting curves.

### Circular dichroism spectra (CD)

Circular dichroism spectra were recorded on a Jasco J-600A spectropolarimeter using 1 mL quartz cuvettes with 5 mm path length. Oligonucleotides (3 μM) were dissolved in a buffer solution consisting of sodium cacodylate (10 mM), EDTA (0.1 mM), and $MgCl_2$ (50 mM) at pH 7.2. All samples were heated for 2 minutes at 90 °C and slowly cooled to room temperature before data collection. Measurements were performed at 20 °C in the 200–350 nm wavelength range with a continuous scanning mode, 50 nm $min^{-1}$ as a scanning speed, 4 s for a response and accumulation 5 times. The spectrum of the buffer solution was subtracted from the sample spectra.

### Molecular modeling

Molecular modeling was performed with Macro Model v9.1 from Schrödinger. All calculations were conducted with AMBER* force field and the GB/SA water model. The dynamic simulations were performed with stochastic dynamics, a SHAKE algorithm to constrain bonds to hydrogen, time step of 1.5 fs and simulation temperature of 300 K. Simulation for 0.5 ns with an equilibration time of 150 ps generated 250 structures, which all were minimized using the PRCG method with convergence threshold of 0.05 kJ $mol^{-1}$. Patel's structure of the anti-parallel triplex[32] was downloaded from the protein data bank (PDB entry pdb134d), followed by incorporation of the nucleobases $\mathbf{T^L}$, $\mathbf{T^\alpha}$, $\mathbf{C^\alpha}$ and $\mathbf{A^L}$.

## Acknowledgements

The Ministry of Higher Education of Egypt is gratefully acknowledged for a predoctoral channel fellowship to Tamer Kosbar.

## Notes and references

1 L. Pauling and R. B. Corey, *Proc. Natl. Acad. Sci. U. S. A.*, 1953, **39**, 84–97.
2 G. Felsenfeld, D. R. Davis and A. Rich, *J. Am. Chem. Soc.*, 1957, **79**, 2023–2027.
3 V. N. Soyfer and V. N. Potaman, *Triple-Helical Nucleic Acids*, Springer, New York, 1996.
4 (*a*) D. Praseuth, A. L. Guieysse and C. Helene, *Biochim. Biophys. Acta*, 1999, **1489**, 181–206; (*b*) M. Duca, P. Vekhoff, K. Oussedik, L. Halby and P. B. Arimondo, *Nucleic Acids Res.*, 2008, **36**, 5123–5138; (*c*) M. Faria and C. Giovannangeli, *J. Gene Med.*, 2001, **3**, 299–310.
5 (*a*) W. M. Olivas and L. J. Maher, *Biochemistry*, 1995, **34**, 278–284; (*b*) A. J. Cheng, J. C. Wang and M. W. Van Dyke, *Antisense Nucleic Acid Drug Dev.*, 1998, **8**, 215–225.
6 W. M. Olivas and L. J. Maher, *Nucleic Acids Res.*, 1995, **23**, 1936–1941.
7 P. B. Arimondo, F. Barcelo, J. S. Sun, J. C. Maurizot, T. Garestier and C. Helene, *Biochemistry*, 1998, **37**, 16627–16635.
8 F. Svinarchuk, D. Cherny, A. Debin, E. Delain and C. Malvy, *Nucleic Acids Res.*, 1996, **24**, 3858–3865.
9 J. M. Dagle and D. L. Weeks, *Nucleic Acids Res.*, 1996, **24**, 2143–2149.
10 O. Doluca, A. S. Boutorine and V. V. Filichev, *ChemBioChem*, 2011, **12**, 2365–2374.
11 J. Lopez de la Osa, C. Gonzalez, R. Gargallo, M. Rueda, E. Cubero, M. Orozco, A. Avino and R. Eritja, *ChemBioChem*, 2006, **7**, 46–48.
12 (*a*) N. Spackova, E. Cubero, J. Sponer and M. Orozco, *J. Am. Chem. Soc.*, 2004, **126**, 14642–14650; (*b*) V. M. Marathias, M. J. Sawicki and P. H. Bolton, *Nucleic Acids Res.*, 1999, **27**, 2860–2867; (*c*) T. S. Rao, R. H. Durland, D. M. Seth, M. A. Myrick, V. Bodepudi and G. R. Revankar, *Biochemistry*, 1995, **34**, 765–772; (*d*) J. E. Gee, G. R. Revankar, T. S. Rao and M. E. Hogan, *Biochemistry*, 1995, **34**, 2042–2048.
13 T. S. Rao, A. F. Lewis, R. H. Durland and G. R. Revankar, *Tetrahedron Lett.*, 1993, **34**, 6709–6712.
14 J. F. Milligan, S. H. Krawczyk, S. Wadwani and M. D. Matteuci, *Nucleic Acids Res.*, 1993, **21**, 327–333.
15 T. S. Rao, A. F. Lewis, T. S. Hill and G. R. Revankar, *Nucleosides Nucleotides*, 1995, **14**, 1–12.

 

16 Y. Aubert, L. Perrouault, C. Helene, C. Giovannangeli and U. Asseline, *Bioorg. Med. Chem.*, 2001, **9**, 1617–1624.
17 (*a*) A. A. Koshkin, S. K. Singh, P. Nielsen, V. K. Rajwanshi, R. Kumar, M. Meldgaard, C. E. Olsen and J. Wengel, *Tetrahedron*, 1998, **54**, 3607–3630; (*b*) S. Obika, D. Nanbu, Y. Hari, J. Andoh, K. Morio, T. Doi and T. Imanishi, *Tetrahedron Lett.*, 1998, **39**, 5401–5404; (*c*) B. Vester and J. Wengel, *Biochemistry*, 2004, **43**, 13233–13241.
18 V. K. Rajwanshi, A. E. Hakansson, B. M. Dahl and J. Wengel, *Chem. Commun.*, 1999, 1395–1396.
19 M. D. Sorensen, L. Kvarno, T. Bryld, A. E. Hakansson, B. Verbeure, G. Gaubert, P. Herdewijn and J. Wengel, *J. Am. Chem. Soc.*, 2002, **124**, 2164–2176.
20 K. M. E. Nielsen, M. Petersen, A. E. Hakansson, J. Wengel and J. P. Jacobsen, *Chem. – Eur. J.*, 2002, **8**, 3001–3009.
21 M. Petersen, C. B. Nielsen, K. E. Nielsen, G. A. Jensen, K. Bondensgaard, S. K. Singh, V. K. Rajwanshi, A. A. Koshkin, B. M. Dahl, J. Wengel and J. P. Jacobsen, *J. Mol. Recognit.*, 2000, **13**, 44–53.
22 S. Obika, Y. Hari, T. Sugimoto, M. Sekiguchi and T. Imanishi, *Tetrahedron Lett.*, 2000, **41**, 8923–8927.
23 J. S. Lee, M. L. Woodsworth, L. J. P. Latimer and A. R. Morgan, *Nucleic Acids Res.*, 1984, **12**, 6603–6614.
24 S. Obika, T. Uneda, T. Sugimoto, D. Nanbu, T. Minami, T. Doi and T. Imanishi, *Bioorg. Med. Chem.*, 2001, **9**, 1001–1011.
25 E. Brunet, P. Alberti, L. Perrouault, R. Babu, J. Wengel and C. Giovannangeli, *J. Biol. Chem.*, 2005, **280**, 20076–20085.
26 A. A. Koshkin, *Tetrahedron*, 2006, **62**, 5962–5972.
27 A. Avino, E. Cubero, C. Gonzalez, R. Eritja and M. Orozco, *J. Am. Chem. Soc.*, 2003, **125**, 16127–16138.
28 C. Dagneaux, H. Gousset, A. K. Shchyolkina1, M. Ouali, R. Letellier, J. Liquier, V. L. Florentiev and E. Taillandier, *Nucleic Acids Res.*, 1996, **24**, 4506–4512.
29 M. G. Grimau, A. Avino, R. Gargallo and R. Eritja, *Chem. Biodiversity*, 2005, **2**, 275–285.
30 K. Bondensgaard, M. Petersen, S. K. Singh, V. K. Rajwanshi, R. Kumar, J. Wengel and J. P. Jacobsen, *Chem. – Eur. J.*, 2000, **6**, 2687–2695.
31 A. Shibata, Y. Ueno, M. Iwata, H. Wakita, A. Matsuda and Y. Kitade, *Bioorg. Med. Chem. Lett.*, 2012, **22**, 2681–2683.
32 I. Radhakrishnan and D. J. Patel, *Structure*, 1993, **1**, 135–152.
33 P. M. D. Moreno, S. Geny, Y. V. Pabon, H. Bergquist, E. M. Zaghloul, C. S. J. Rocha, I. I. Oprea, B. Bestas, S. EL Andaloussi, P. T. Jørgensen, E. B. Pedersen, K. E. Lundin, R. Zain, J. Wengel and C. I. Edvard Smith, *Nucleic Acids Res.*, 2013, **41**, 3257–3273.